Phase-separation technologies for 3D scaffold engineering

5

Panagiotis Sofokleous, Matthew H.W. Chin and Richard Day
University College London, London, United Kingdom

5.1 Introduction

5.1.1 Porous scaffold technologies in tissue engineering

In tissue engineering, porous scaffolds are often required to provide mechanical support responsible for tissue formation and specific structural features. Depending on the intended role of the tissue engineered construct, different scaffolding requirements might be needed at any stage during manufacturing, delivery, or function of the construct. For example, this can include the initial stages of cell isolation through tissue growth, maturation, and in vivo delivery of the tissue-engineered construct.

Porous tissue scaffolds offer several benefits for the engineering of soft tissues. These most notably include infiltration of cells and tissue together with vascularization to support perfusion of oxygen and nutrients. Scaffolds intended for tissue engineering have been fabricated using a range of techniques such as coagulation, compression molding, and salt leaching, in which salt crystals are used as the porogen in a polymer matrix. The salt is then subsequently washed off (leached) to leave a porous polymeric scaffold [1].

Another platform technology to produce porous biomaterials is called thermally induced phase separation (TIPS). It is a thermodynamic phenomenon commonly exploited to produce porous polymeric membranes [2]. The advantage of using TIPS over salt leaching is that a higher control over pore size consistency can be achieved. The structure of TIPS-derived materials exhibits a highly interconnected, porous architecture that can be tuned and is ideal for tissue ingrowth [3]. Due to these properties, the technology has recently been employed to manufacture porous hierarchical materials (materials that exhibit structure on more than one length scale; the structural elements of a material themselves have structure, for example the structural element of a porous material are mostly spherical pores) [4–8]. The porous structural hierarchy of a material can play a large part in determining the bulk material properties and in turn defining the final properties of the tissue scaffold [9].

5.1.2 Short historical overview of TIPS process

Van der Waals provided the first qualitative description of the partial miscibility of polymer solutions on the basis of his equation of state [10]. Because of the huge

Functional 3D Tissue Engineering Scaffolds. DOI: http://dx.doi.org/10.1016/B978-0-08-100979-6.00005-7

differences in the molecular size of the polymer solution components, he was able to assign the extreme asymmetric shape of the coexistence curves in their systems. A better understanding of the lattice theory of polymer solutions, mainly done by Flory [11] and Huggins [12], introduced a more quantitative approach of the partial miscibility of polymer solutions. The Flory−Huggins model stated that the variance in molecular size between the components is responsible for the shift of the two-phase region towards the solvent axis. In 1949, Tompa [13] calculated the ternary phase diagrams on the basis of the Flory−Huggins theory, hence offering to the research community a better understanding of the actual polymer solution systems. Because of the detailed phase diagrams provided by the Flory−Huggins theory the differences between ternary and binary systems were revealed. Ternary phase diagrams represent the phase behavior of mixtures containing three components (e.g., concentration, temperature, and pressure) in a triangular diagram [14]. A binary phase diagram is a temperature−composition diagram that describes the equilibrium phases existing at a given temperature and composition. The equilibrium state can be found from the Gibbs free energy dependence on temperature and composition [15,16]. The Flory−Huggins model revealed the ternary phase diagrams for the blends of one solvent component and two homologous polymers differing in chain length only [17]. For low-molecular-weight polymer solution systems these differences were described qualitatively by Schreinemakers [18,19].

5.2 Phase-separation technologies for 3D scaffolds

5.2.1 *Thermal induced phase-separation technique (TIPS) for polymers*

In recent years, the thermally induced phase separation (TIPS) process has been used extensively to form porous materials, such as scaffolds [20] and drug delivery devices [21] with pore sizes ranging from the nano- to the micro-scale. A porous microstructure with well-defined pore size and interconnected channels offer ideal features for tissue-engineering scaffolds [22]. Furthermore, many advanced drug-delivery devices such as particles and fibers require a porous structure that can offer high encapsulation efficiency, easy control over pore size, and a more predictable degradation mechanism [4].

In comparison with other conventional methods, TIPS process can form intrinsically interconnected porous networks in one simple, inexpensive, and controllable process. Also, a wide variety of polymers can be used in the TIPS technique, even ones that have low solubility [21]. This can allow the preparation of membranes from semi-crystalline polymers, something that cannot be achieved via the traditional nonsolvent-induced phase inversion method [2]. Furthermore the products' characteristics such as the morphology and pore size made by the TIPS technique can be easily controlled by adjusting the process parameters, including the polymer concentration, quenching temperature, quenching period, solvent/nonsolvent ratio, and surfactant addition [21]. This allows the production of a variety of

microstructures such as relatively thick isotropic microporous structures applicable for controlled release [2].

Thermally induced phase separation is a thermodynamic technique that involves the separation of phases due to physical incompatibility. To be more specific, a homogeneous polymer solution will form a polymer-rich and a polymer-lean phase as it becomes thermodynamically unstable when certain temperature conditions are applied. When the solvent is removed, the polymer-rich phase will form a solid 3D structure while the polymer-poor phase will become the pores (void space) of that arrangement [23]. Specifically, the TIPS technique uses the thermal energy as a driving force to separate the polymer solution into the two different phases, either by exposing the solution to an immiscible solvent or by cooling the solution below its solubility temperature. It is therefore preferable to use solvents with a relatively high melting temperature such as dioxane or dimethyl carbonate [21].

In its more basic form, the TIPS process involves the following steps [2,21,24]:

1. A homogenous polymer solution (or melt-blend) is prepared by melt blending or dissolving the polymer with a high boiling, low molecular weight liquid or solid referred to as the diluent (raw material dissolution).
2. The polymer solution or melt-blend is then cast or extruded into the preferred shape.
3. The thermal energy is removed to induce phase separation and crystallization of the polymer (the solution is cooled down to the desired quenching temperature).
4. The diluent is removed (typically by solvent extraction). The diluent is evaporated by freeze-drying or freeze-extraction to insure complete solvent removal and yield a microporous structure.

There are two main phase separation mechanisms in the TIPS process, depending on the polymer−diluent interactions. A strong polymer−solvent interaction leads to solid−liquid phase separation, where the polymer crystallizes from the melt-blend. A weak polymer−solvent interaction will lead to liquid−liquid phase separation, where a formation of a polymer-rich liquid matrix and a dispersed polymer-poor liquid, followed by solidification of the polymer [24]. For example, a liquid−liquid phase separation is formed if the degree of polymer−solvent interaction is decreased by adding a nonsolvent in the polymer/solvent mixture [21].

5.2.1.1 Parameters affecting the TIPS process

The final structure produced using the TIPS process (e.g., porosity) can be readily altered by changing the processing parameters such as polymer type and concentration, solvent composition, quenching temperature and time, coarsening, etc. Below we explain briefly how each of these parameters is affecting the final product in the TIPS process.

Polymer type: The targeted application that is of interest will determine the type of polymer that can be used. The polymer chemistry, molecular weight, solubility, hydrophilicity/hydrophobicity, degradation/erosion mechanism, etc., are all important parameters that must be taken in consideration before producing the TIPS materials [21,25]. For example

in the case of drug delivery device in vivo it is preferable to use a biodegradable polymer that can degrade after a specific time period or after it has delivered the necessary compound to the target side [26]. The most common polymers used in the TIPS process are PLGA and PLLA and each one will give different morphologies, if the same process parameters are used. This is due to the fact that the amorphous PLGA rearranges more easily and is less stable than the semi-crystalline PLLA during freeze drying [27].

Polymer concentration: The morphology of the TIPS materials is greatly affected from this parameter. When the concentration of the polymer is high enough then the porosity of the material is decreased if compared with lower polymer concentrations [21]. Also when the polymer concentration is below a critical point, where the polymer-lean phase is the dominant phase, then the porous material produced is collapsing upon solvent removal due to the dispersion of polymer-rich droplets throughout the polymer-lean matrix [28]. By using specific polymer concentrations in the solid−liquid phase separation process, bundles of channels or anisotropic ladder-like structures can be formed because of the specific alignment induced by the crystallization of the solvent [29,30].

Solvent composition: Use of a solvent/nonsolvent mixture instead of a mono-solvent affects the formation of scaffolds. By adding water in a solvent system, the morphology of the porous material changes drastically [21]. Wei and Ma [31] proved that by adding small amounts of water in a solvent system (<5%) the pore size of the TIPS material was decreased from 100 to 10 μm and the ladder-like pore morphology was replaced by a random one. Also the mechanical properties of a TIPS material can be affected by the ratio of the solvent/nonsolvent mixture. For example the compressive modulus of a porous TIPS scaffold formed can be reduced when using a solvent/nonsolvent system due to the fact that the regular and orientated pore structures can be replaced by random pore morphology if compared to a monosolvent [21,31].

Quenching temperature and time: When the temperature of the polymer solution drops below the melting point of the solvent (dioxane: 11.8°C, dimethyl carbonate (DMC): 2−4°C), then crystallization of the solvent occurs, which leads to the separation of the polymer and solvent that also leads to the polymer-rich and polymer-lean phase [32]. A beadlike or isolated cellular structure is noticed when the system is quenched into the metastable region, due to the nucleation and growth mechanism of the phase-separation process [28]. When the polymer system is cooled down at a faster rate and in a shorter period of time (e.g., immersed in liquid nitrogen [LN_2]: −195.79°C), as a result of very low quenching temperatures, then fewer crystals are formed in its structure and the solvent nucleation and phase separation occurs in a shorter time. This leads to the formation of smaller pores in the TIPS material. Higher quenching temperatures support larger crystals formation and lead to larger pore sizes [21].

Coarsening: When the interfacial free energy associated with the interfacial area is decreased under a certain point then coalescence can occur between the phase-separated droplets, hence leading to higher pore sizes in the TIPS material. This can happen when the coarsening effect is used at the late stage of phase separation and by setting the temperature accordingly (depending on the polymer-solution system used) as it plays an important role in the coarsening effect. The coarsening effect can be accomplished below the phase-separation temperature of the polymer-solution system, but at a temperature above the solidification temperature of the solvent.

Cloud point temperature: This is the temperature at which a clear polymer solution turns turbid and it must be measured experimentally for each polymer-solution system independently by plotting the cloud point curve (Temperature $= f$ (Polymer concentration)). By adding a nonsolvent in the system the cloud point temperature changes. For example

if the water content is increased in a PLGA\dioxane mixture then the cloud point temperature increases [33]. In general the cloud point temperature decreases as the polymer concentration, water presence, and the molecular weight of the polymer decreases. When the polymer concentration and the molecular weight of the polymer decreases, the cloud point temperature decreases because of higher interaction between the polymer−solvent mixture [21,34].

5.2.1.2 Basic thermodynamics of TIPS process

The Gibbs free energy of mixing

The Gibbs free energy of mixing describes how spontaneous is the process of mixing two solutions at constant (absolute) temperature and (external) pressure and is given by the following relation [35]:

$$\Delta G_m = \Delta H_m - T\Delta S_m \tag{5.1}$$

where Δ, represents a change and is the value of a variable for a solution or mixture minus the values for the pure components considered separately; ΔH_m, enthalpy of mixing; and ΔS_m, entropy of mixing.

For ideal solutions the enthalpy of mixing is considered zero ($\Delta H_m = 0$) and the Gibbs free energy of mixing is always negative, which means that the two solutions are mixing instantaneously. For regular solutions a positive enthalpy of mixing mostly means that the solutions are immiscible.

The Flory−Huggins model [11,12,36,37]

The Flory−Huggins (F−H) equation is a mathematical model that describes the thermodynamic interactions between polymer/solvent systems when polymers with different molecular sizes are used and the entropy and enthalpy of mixing in these systems is taken in consideration. In general, the F−H model is an expression of the Gibbs free energy of mixing (Eq. 5.1) of a number of linear macromolecular homologous components in a single solvent, which describes the change ΔG_m of the Gibbs free energy when a polymer is mixed with a solvent. Although is a simple model, it offers useful results for interpreting experiments [38,39].

By using the Gibbs free energy equation and taking into account the following assumptions we can get the F−H equation, which can be valuable in calculating useful experimental data about the polymer/solvent system.

If assumed that each polymer segment (monomer of the polymer chain) and each solvent molecule occupy each only one site on the lattice so that the dissymmetry in molecular sizes is taken into account then the total number of sites is:

$$N = N_1 + yN_1 \tag{5.2}$$

where N_1, number of solvent molecules; N_2, number of polymer molecules; and y, number of segments that each one has.

The entropy of mixing ΔS_m for a polymer system is calculated by:

$$\Delta S_m = -k\left[N_1 \ln\left(\frac{N_1}{N}\right) + N_2 \ln\left(y\frac{N_2}{N}\right)\right] \tag{5.3}$$

where k is the Boltzmann's constant.

If the lattice volume fractors are also represented as below:

$$\begin{aligned} \vartheta_1 &= \frac{N_1}{N} \\ \vartheta_2 &= y\frac{N_2}{N} \end{aligned} \tag{5.4}$$

then $\Delta S_m = -k[N_1 \ln(\vartheta_1) + N_2 \ln(\vartheta_2)]$

Eq. (5.4) shows that there is an entropy change in the polymer solution system and because of that is expected a change in the enthalpy. To calculate the enthalpy change three molecular interactions must be consider: solvent−solvent w_{11}, monomer−monomer w_{22} (not the covalent bonding, but between different chain sections), and monomer−solvent w_{12}. Each of these interactions occurs at the expense of the average of the other two, so the energy increase per monomer−solvent interaction can be described as:

$$\Delta w = w_{12} - \frac{1}{2}(w_{22} + w_{11}) \tag{5.5}$$

The total number of such contacts is:

$$yN_2z\vartheta_1 = N_1\vartheta_2 z \tag{5.6}$$

where z, coordination number, which describes the number of nearest neighbors for a lattice site, each one occupied either by one polymer chain segment or a solvent molecule; yN_2, total number of polymer segments (monomers) in the solution; and yN_2z, number of nearest-neighbor sites to all the polymer segments.

The enthalpy change is equal to the energy change per polymer monomer−solvent interaction multiplied by the number of such interactions and is represented by Eq. (5.7):

$$\Delta H_m = N_1\vartheta_2 z\Delta w \tag{5.7}$$

The polymer−solvent interaction parameter y is defined as:

$$y_{12} = \frac{z\Delta w}{kT} \tag{5.8}$$

y_{12} depends on the nature of both the solvent and the solute, and is the only material-specific parameter in the model. If it is large and positive, ΔG_m becomes positive and demixing occurs [40].

Hence the enthalpy change becomes:

$$\Delta H_m = kTN_1\vartheta_2 y_{12} \tag{5.9}$$

and demixing occurs.

Assembling terms, the total free energy change when a polymer solution is mixed with a solvent is:

$$\Delta G_m = RT(n_1 \ln \vartheta_1 + n_2 \ln \vartheta_2 + n_1\vartheta_2 y_{12}) \tag{5.10}$$

where the expression from molecules N_1 and N_2 was altered to moles n_1 and n_2 by transferring Avogadro's number N_A to the gas constant $R = kN_A$. The subscripts n_i refer to nonsolvent n_1, solvent n_2, and polymer (n_3) [41].

Eq. (5.10) is the Gibbs free energy of mixing as defined for polymer/oligomer systems.

Evaluation of the classic Flory–Huggins theory, currently used as the thermodynamic basis for the TIPS process indicated that this theory sometimes does not accurately describe the polymer/diluent system behavior because the free volume effect is not considered. The polymer/diluent system is expected to have significant free volume effects due to the dissimilarity of equation of state (EOS) properties of the polymer and diluent. Many research articles were published since then based on the initial Flory–Huggins model in order to give a more accurate description of the thermodynamic assessments of binary phase diagrams in organic and polymeric systems [39,42,43].

Phase equilibria and miscibility in liquid polymer systems

The Gibbs free energy of mixing ΔG_m (see Eq. 5.1) and its second derivatives with relevance to polymer volume fraction θ_2, at a fixed temperature T and pressure P, can provide the conditions for miscibility in any two component polymer/diluent system [12]. The conditions are as follows:

$$\Delta G_m < 0 \quad \text{(Condition 1)}$$
$$\left(\frac{\vartheta^2(\Delta G_m)}{\vartheta(\theta_2)^2}\right)_{T,P} > 0 \quad \text{(Condition 2)}$$

If none of the above criteria is met then the solution may separate into two phases in equilibrium. Three main different cases can be achieved and they are as follows [40]:

1. Immiscibility throughout the composition range $0 \le \theta_2 \le 1$ (both conditions not met). The solution may separate into two phases in equilibrium.
2. Partial miscibility (condition 1 is met but condition 2 is not—immiscibility within the composition range indicated by a negative second derivative)
3. Miscibility across the entire composition range (both conditions met).

Critical solution temperature (CST)

Polymer systems with specific polymer concentration that experience phase separation as the temperature is decreasing can have an upper critical solution temperature (UCST). This is the maximum temperature at which a two-phase liquid−liquid mixture can exist. Systems that experience phase separation as the temperature is increasing can have a lower critical solution temperature (LCST) [44,45].

At high temperatures, there is plenty of thermal energy to achieve dissolution at the entire polymer solution composition. As the temperature is reduced and thermal energy is converting to another form (mostly removed from the system), the strength of the polymer/diluent interactions is reduced. Hence, the polymer and the diluent molecules withdraw from each other, and phase separation follows within the polymer system bracketed by the cotangential points (equilibrium phases of equal chemical potential) [40].

5.2.2 Solid−liquid and liquid−liquid phase separation

The most important factor responsible on whether a liquid−liquid (L−L) or solid−liquid (S−L) phase-separation process takes place in a semi-crystalline polymer system is the miscibility of the system. Miscibility in TIPS process can be quantified depending on how strongly the semi-crystalline polymer interacts with the diluent in the polymer/diluent system [40,42]. S−L phase separation occurs when the interaction between polymer/diluent is strong and it happens via polymer crystallization when cooled (when high initial polymer concentration is used) [46]. L−L phase separation occurs when the interaction between polymer/diluent is weak (when low initial polymer concentration is used). In this case the system becomes unstable by showing UCST behavior when cooled [47]. In general when the binodal line, is found above the crystallization temperature (T_f), L−L phase separation occurs. When the crystallization temperature is higher than the binodal line, S−L phase separation occurs (Fig. 5.1) [42,48].

5.2.2.1 Solid−liquid phase separation

S−L phase separation usually occurs because of crystallization of the polymer in a homogeneous solution or because of solvent crystallization [44].

The route that TIPS follows is dictated by the relationship between the solvent crystallization temperature (or the freezing point, (T_f) and the critical solution temperature (T_c)). Here, the criterion of $T_f > T_c$ will need to be fulfilled in order for S−L phase separation to happen. In this case, when the temperature of a homogeneous polymer solution is lowered to a value between T_f and T_c, the solvent crystallizes before L−L phase separation can take place (i.e., the process shown in Fig. 5.1(i) will not occur) [48]. As the solvent solidifies the polymer essentially gets forced out of the solution, leading to S−L demixing. A porous structure will then be formed in the resultant polymeric scaffold after extraction of the crystallized solvent by sublimation under vacuum (lyophilization) [2,34,48]. It should be noted that the crystallization process has a direct impact on the final morphology of

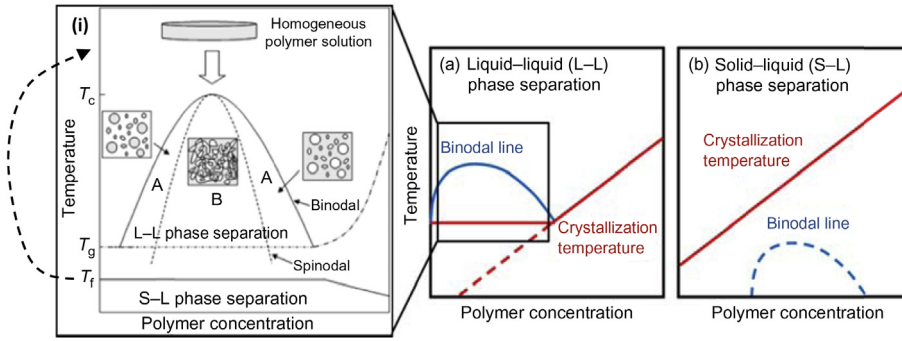

Figure 5.1 Temperature−composition phase diagrams for a polymer−solvent system with an upper critical solution (T_c) temperature undergoing (a) L−L phase separation and (b) S−L phase separation via polymer crystallization. The crystallization temperature in (a) and (b) refers to that of the polymer. Diagram (i) is the box-bounded region within (a) and it shows that T_c is the highest temperature at which L−L phase separation occurs, hence "upper" T_c. T_g is the glass-transition temperature of the polymer solution and T_f the solvent freezing point. In the case of S−L TIPS via solvent crystallization, T_f is above T_c as indicated by the dashed arrow in (i).
Source: Panel (i) adapted from L. He, et al., Microstructural characteristics and crystallization behaviors of poly (L-lactide) scaffolds by thermally induced phase separation, J. Appl. Polym. Sci. 131 (4) (2014), Copyright 2013, with permission from John Wiley & Sons. Panels (a) and (b) reproduced from T. Ishigami, et al., Solidification behavior of polymer solution during membrane preparation by thermally induced phase separation, Membranes 4 (1) (2014) 113−122.

the scaffold because pores that are left behind will possess a silhouetted resemblance of the solvent crystallites. Therefore, the solvent has the roles of dissolving the polymer and acting as a porogen, hence affecting directly the size and distribution of the pores, as well as the structural integrity of the TIPS material [24,49].

In the solid−liquid TIPS process, process parameters can be optimized in order to control the TIPS material structure. Some of these parameter are the dissolution temperature T_d, at which the melt-blend is formed, the isothermal crystallization temperature T_c, at which the melt-blend is crystallized, the polymer concentration etc. [21,24,44].

5.2.2.2 Liquid−liquid phase separation

When the polymer/diluent system is thermodynamically unstable, then L−L phase separation occurs and the formation of a polymer-rich and polymer-poor phase is observed within the polymer/diluent system. The polymer poor phase is then removed by freeze drying or freeze-extraction to insure complete solvent sublimation, hence leaving behind a highly porous polymer material [24]. This can take place in crystalline or glassy polymeric systems [50]. There are two possible ways to get L−L phase separation in a polymeric system: (1) with a temperature dropped

in order to increase the number of disadvantageous polymer/diluent interactions and (2) by elevating the temperature to increase the free volume [44].

The cooling temperatures used at the polymer/diluent system are very important for determining the final morphology of the TIPS material in L−L phase. At temperatures just below the critical temperature (T_c) or cloud point in the case of polydisperse polymers the phase separation occurs via a nucleation and growth mechanism [48]. At lower temperatures below the spinodal curve as shown in Fig. 5.1(i), the separation take place via spinodal decomposition. While the nucleation and growth mechanism results in spheroidal domains, spinodal decomposition causes the formation of interconnected pores [50].

Many parameters affect the final TIPS material pore morphology formed in the L−L phase such as the polymer concentration, the cooling method and time, the solvent/nonsolvent ratio and the presence of surfactants [21,33,51,52].

5.2.2.3 Binodal and spinodal curve in TIPS process

As mentioned before the production of the TIPS-derived polymeric materials essentially exploits changes in thermal energy to drive a homogeneous polymer solution into a biphasic system [21]. There are two curves in a typical temperature composition phase diagram for a polymer/solvent system and they are unique for each system. These curves are called a binodal and a spinodal curves. This is perhaps best explained with the temperature-concentration phase diagram in Fig. 5.1(i).

The plot shows a border known as the binodal curve, above which the solution is homogeneous and below which liquid−liquid demixing occurs. To be more specific the binodal curve represents the thermodynamic equilibrium of liquid−liquid demixing. The demixing is due to the thermodynamic instability and unfavorable polymer−solvent interactions within the system caused by the drop in temperature [32]. When a polymer solution is quenched below its binodal solubility curve, a polymer-rich phase and a polymer-lean phase are created. For each single polymer, the binodal can be shifted to higher temperatures when the polymer concentration is fixed or to a higher polymer concentration when the temperature is fixed by selecting a less compatible diluent [40].

In addition, there is another curve in the phase diagram called the spinodal curve, below which is the unstable region and the composition of the system assumes a bicontinuous morphology [39]. The spinodal curve is the line where the Gibbs free energy of mixing second derivative equals to zero, and it splits the two-phase region into two zones. The area below the spinodal curve is the unstable region, and the area located in the zone between the binodal and spinodal curves is the metastable region. The terms unstable and metastable state the solution's capability to resist phase separation [45]. L−L demixing in the metastable region displays a poor connected stringy or beady morphology, but if the system is into the unstable region then L−L phase separation occurs that results in a well-interconnected porous structure [40]. If an open and well interconnected porosity it is desirable then the temperature must drop below the spinodal curve. This is the region where the defined interconnected pore structure of a polymer material is formed and the mechanism by which it happens is called spinodal decomposition [53]. After the separation, the solvent can be removed via freeze drying.

Depending on the parameters used (temperature, quench rate, polymer concentration) different porous morphologies can be created [21,53].

The point where the structure and amounts of the polymer-rich phase and the polymer-lean phase become very similar is called critical point. Critical point is where the binodal and spinodal merge and for a monodisperse polymer, this point is located at the maximum of the binodal line (see Fig. 5.1(i)) [32]. This point is unique for each polymer/diluent system and satisfies the following three criteria:

$$\left(\frac{\vartheta^2(\Delta G_{\mathrm{m}})}{\vartheta(\theta_2)^2}\right)_{T,P} = 0 \quad \text{(Criteria 1)}$$

$$\left(\frac{\vartheta^3(\Delta G_{\mathrm{m}})}{\vartheta(\theta_2)^3}\right)_{T,P} > 0 \quad \text{(Criteria 2)}$$

$$\left(\frac{\vartheta^4(\Delta G_{\mathrm{m}})}{\vartheta(\theta_2)^4}\right)_{T,P} = 0 \quad \text{(Criteria 3)}$$

The critical temperature and critical polymer concentration represent the critical point value and the critical interaction parameter at that point is also used as a condition of system miscibility. Both points depend on the size of the polymer and diluent molecules [40,45].

5.3 Three-dimensional scaffold preparation by TIPS process

5.3.1 Tissue engineering scaffolds by TIPS process

Scaffolds manufactured using phase separation techniques offer several attributes ideally suited for tissue-engineering applications. Firstly, the technique provides an approach for achieving scaffolds with bespoke hierarchical structures that provide optimized topographical features and porosity. The appropriate matching of these features to different cell types intended to interact with the scaffold is critical for achieving efficient cell attachment and long-term viability of the tissue-engineered construct. In addition to this, the anisotropic (the material's directional dependence of a physical property) pore structures can be exploited to provide conduits for cell guidance or provide anisotropic mechanical strength to the scaffold. The size, shape and arrangement of the pores formed in the material can change the scaffolds' physical properties. Mechanical strength can be further enhanced by manufacturing scaffolds from polymer composites, which may also be utilized to improve bioactivity of the scaffold. Phase separation therefore provides an unrivaled manufacturing process for producing scaffolds designed for specific tissue-engineering applications.

Liquid−liquid phase separation has been applied to the development of porous polymeric scaffolds composed of biodegradable polymers that resemble the natural extracellular matrix. Yang and colleagues developed PLLA nano-structured scaffolds using this approach for the culture of nerve stem cells (NSCs) that could be used for nerve tissue engineering [54]. The scaffold fiber diameters ranged in size from 50 to

350 nm. Control of fiber diameter, porosity and surface area to volume was achieved by adjusting the concentration of the polymer solution. The in vitro performance of the NSCs on the nano-fibrous scaffolds was investigated and reported to support NSC differentiation and provide a positive cue for neurite outgrowth.

Improved biocompatibility often attributed to natural polymers such as chitosan can also be harnessed with scaffolds fabricated using phase-separation technologies. Whilst three dimensional scaffolds can be readily prepared by conventional lyophilization of chitosan solutions, the resulting porous structures often have low interconnectivity and have been associated with poor cell affinity. To overcome this limitation, Lim and colleagues explored the use of liquid−liquid or liquid−solid phase separation to produce three-dimensional porous chitosan-polyvinyl pyrrolidone (PVP) scaffolds [55]. Freeze dried scaffolds were prepared from a mixture of an acidic aqueous solution with butanol as a nonsolvent and a chitosan-PVP quaternary system (a system that represents the phase behavior of mixtures containing four components in a pyramid-shaped diagram). Cell-affinity measurements performed by culturing NIH-3T3 cells on scaffolds prepared with PVP revealed enhanced cell adhesion and proliferation compared with the chitosan phase-separation scaffolds containing no PVP. The authors attributed this effect to the open structure and minute pores between the main pores, along with good mass transfer due to the open structure achieved with the chitosan-PVP scaffolds produced via phase separation from a quaternary system.

Increased porosity and interconnectivity of tissue-engineering scaffolds can also be achieved by combining liquid−liquid phase separations for polymer solutions with inclusion of particulates, such as salt, that is subsequently washed out. Heijkants and colleagues successfully used this approach to create foam scaffolds with high interconnectivity and porosity and the correct compression modulus suitable for application to the knee for tissue engineering of meniscus like tissue in orthopedic applications [56]. When implanted into a pre-clinical model of meniscus regeneration, the very open porous structure allowed tissue to infiltrate deep into the structure. After 6 months the mechanical properties of the newly formed tissue was comparable to native meniscus tissue.

The biophysical cues provided by scaffolds fabricated using phase separation to enhance stem cell differentiation has also been described [57]. Liquid−liquid and solid−liquid phase separation of poly(D,L-lactic acid) (PDLLA) dissolved in dioxane was used to produce scaffolds designed to differentiate mouse embryonic stem cells into neural cells. Cells cultured on the 3D porous scaffolds expressed a significantly greater number of neural markers compared with those cultured on 2D substrates. Furthermore, differentiated cells exhibited neurite outgrowth and were observed migrating through the scaffold structure.

The structural stability of scaffolds produced via phase separation can be improved by using composite polymers that consist of the addition of solid particulate. This has been demonstrated by Arahira and Todo, who investigated the effect of incorporating β-tricalcium phosphate (TCP) on the compressive mechanical behavior of collagen scaffolds produced via solid−liquid phase separation, along with the behavior of rat mesenchymal stem cells (rMSCs) cultured on the scaffolds

over 28 days [58]. The composite scaffolds containing TCP had a continuous porous structure with pore sizes ranging from 50 to 150 μm. Rat MSCs cultured one the scaffolds had higher ALP activity and increased expression of osteoblastic markers compared with scaffolds consisting of collagen only. The compressive modulus of the composite scaffold was affected by both the material degradation and the proliferation of cells and the ECM formation, which occurred over three distinct stages. The initial increase in modulus of the scaffold was associated with cell proliferation, followed by a decrease caused by scaffold degradation. During the final stage the modulus was restored due to formation and growth of mineralized nodules causing calcification of the scaffold.

Mechanical strength of tissue-engineering scaffolds is particularly important for bone applications. Solid−liquid phase separation has been used to manufacture scaffolds from a variety of polymers that often consist of composite materials to improve mechanical properties and tissue integration [59−61]. The static and dynamic mechanical behavior of composite foams consisting of PDLLA/Bioglass and produced via solid−liquid phase separation has been investigated. Scaffolds containing particulate Bioglass exhibited anisotropic bi-modal pore distribution. Although variation in through thickness of pore morphology and density was observed, the majority of foam structure was homogeneous, consisting of continuous tubular macro-pores interconnected by a micro-porous network. Mechanical anisotropy was found to be concomitant with the direction of the macro-pores and the presence of low volume fractions of Bioglass (<15 vol%) resulted in stiffening of the composites in comparison with pure PDLLA foams [62].

Dziadek et al. also investigated scaffolds composed of composites of poly (e-caprolactone) and silica-rich bioactive glasses prepared by solid−liquid phase separation compared with scaffolds prepared using solvent casting particulate leaching or phase inversion [63]. Distinct differences were observed with the microstructure, crystallinity, degradation rate, and bioactivity of each composite material depending on the fabrication method and composition of the bioactive glasses. The authors suggested that different fabrication methods could be used to control of pore architecture, polymer crystallinity, and biodegradation could be used to influence cell adhesion and proliferation.

The presence of a surface skin caused by interfacial tension during evaporation of the solvent is often associated with freeze-drying methods used with solid−liquid phase separation fabrication processes. Depending on the intended application of the scaffold, this may or may not be of benefit. Therefore, fabrication processes have been devised to eliminate this. A notable example of this is the freeze-extraction method used to produce highly porous and interconnected scaffolds [64]. This approach is feasible with a variety of freezing media. For example, Goh and Ooi describe the use of a dry ice/ethanol bath to produce scaffolds with open scaffold architecture that contain ladder-like structures and interconnected pores.

Refinement of phase separation techniques have also been used to create bespoke shaped scaffolds designed for specific applications. Day and colleagues have described the fabrication of highly porous, biodegradable particles that can be tailored in terms of size and porosity by adjusting processing parameters including

polymer type and concentration, solvent and jetting techniques used [4,65,66]. This technique has been successfully applied for applications including drug delivery and cell therapy [7,67].

Other examples of refining thermally induced phase separation processes include combining it with injection molding. Sundback used this approach with 85:15 poly (DL-lactide-co-glycolide) to fabricate porous, biodegradable conduits with dimensionally toleranced, longitudinally aligned channels designed mimic the structure of peripheral nerves and support the adherence of Schwann cells [68]. The polymer solution was cooled as it was delivered in to the mold that had been pre-chilled in a box of dry ice, resulting in solid−liquid phase separation and the production of macroporous foams with high anisotropy. Semi-permeable skins were formed on the luminal and outer surfaces of the conduit. The use of a mold enabled inexpensive production of scaffolds of variable configurations and dimensions and could be applied to other scaffolds intended for tissue engineering hollow visceral organs.

Hierarchical structures obtained with scaffolds fabricated using thermally induced phase separation can refined using dual solid−liquid phase separation. This approach was used to fabricate a biomimetic poly(propylene carbonate) porous scaffold with a nanofibrous chitosan network contained within macropores intended for bone tissue engineering [69]. The first solid−liquid phase-separation stage consisted of poly(propylene carbonate) with paraffin spheres (300−450 μm in diameter) used as a porogen. The resulting porous scaffold had solid pore walls that exhibited high compressive modulus ideal for providing mechanical support. The second solid−liquid phase-separation stage was achieved by soaking the poly(propylene carbonate) scaffold in a chitosan solution before quenching in liquid nitrogen and lyophilization. The second phase-separation stage introduced a nanofibrous chitosan network into the macropores of the scaffold that resembled extracellular matrix fibrillary collagen.

5.3.2 Applications of solid−liquid phase separation

As mentioned before, given a polymer−diluent system, S−L phase separation can occur via either (A) solvent crystallization or (B) polymer crystallization. This section focuses on porous scaffolds generated by TIPS via mechanism (A), but Fig. 5.1b also provides a brief insight into S−L TIPS via (B).

For biomedical applications, the lyophilization step is especially important in ensuring biocompatibility of the material as residue of commonly used TIPS solvents such as dioxane is toxic and a potential carcinogen [70]. This is also the reason for adopting alternative TIPS solvents that have low toxicity, for example, dimethyl carbonate [4].

One of the major considerations in creating 3D tissue scaffolds is gaining geometric control over the scaffold's porous architecture. This is attributed to the fact that tissue scaffolds act as a source of spatial and mechanical cues, which are sensed by cells via mechanisms such as mechanotransduction. As a result, the pore dimensions can have profound impact on cellular behavior such as adhesion, migration, and differentiation [71−77]. Addressing this engineering challenge, S−L phase separation presents a number of parameters that can be manipulated to

control pore morphology. These parameters include, but are not limited to, the solvent of choice, quenching temperature gradient, quenching rate, quenching duration, and polymer concentration [21,29].

He et al. carried out a study to compare different pore morphologies formed by S−L and L−L phase separation. In the study, S−L phase separation was induced using a binary system of poly(L-lactide)-dioxane (PLLA-dioxane) at −80°C. Addition of a nonsolvent to the polymer solution, on the other hand, promoted L−L phase separation—this was demonstrated using a ternary system of PLLA-dioxane-water under the same conditions [29]. The different porous structures generated from the two mechanisms are shown in Fig. 5.2. In the experiment, S−L phase separation produced an anisotropic channel-like morphology with an internal ladder substructure (Fig. 5.2A), whereas L−L phase separation created an isotropic macropore structure (Fig. 5.2B). Hence, the mechanism via which TIPS occurs can be controlled by modulating the solvent/nonsolvent ratio. As a result, this will bias the fabrication towards the pore morphology typical of the corresponding mechanism.

In fact, anisotropic micro-tubular structures are quite typical of S−L phase separation and the process generally produces bundles of channels in the polymeric matrix with diameter approximately 100 μm. The channels are known to exhibit a preferential orientation dictated by the advancement of the solvent crystallization front, with the long axes parallel to the freezing direction. These characteristics were shown by Schugens et al. using a poly(lactide)-dioxane (PLA-dioxane) system (Fig. 5.3A) [49]. Poly(lactic-co-glycolic) acid (PLGA) TIPS microspheres created by Day et al. [4,78] possess radial topographical patterns and internal ladder substructures (examples indicated by arrows in Fig. 5.4), demonstrating these TIPS-derived patterns can be generated in both 2D membranes and spherical scaffolds.

The highly anisotropic structures generated from S−L phase separation have been found to be useful in nerve and joint cartilage regeneration, as they mimic the

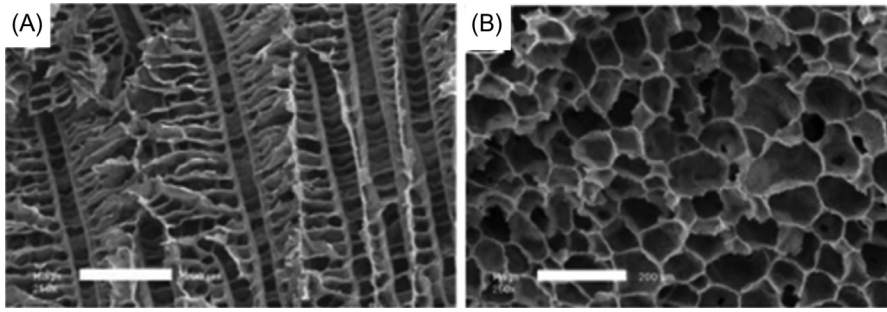

Figure 5.2 Scanning electron microscopy (SEM) images of (A) morphology produced from S−L demixing of PLLA-dioxane and (B) morphology from L−L demixing of PLLA-dioxane-water.
Source: Reproduced from L. He, et al., Microstructural characteristics and crystallization behaviors of poly (L-lactide) scaffolds by thermally induced phase separation, J. Appl. Polym. Sci. 131 (4) (2014), Copyright 2013, with permission from John Wiley & Sons.

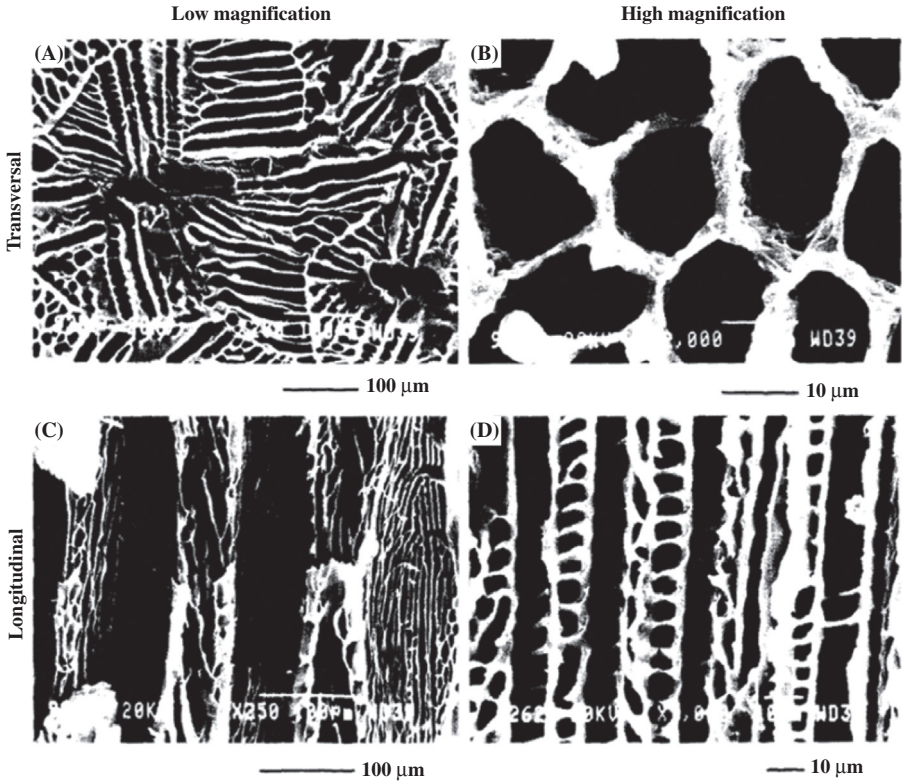

Figure 5.3 SEM images of PLLA foams produced by Schugens et al. via solid−liquid phase separation.
Source: Reproduced from C. Schugens, et al., Biodegradable and macroporous polylactide implants for cell transplantation: 1. Preparation of macroporous polylactide supports by solid−liquid phase separation, Polymer (Guildf) 37 (6) (1996) 1027−1038, Copyright 1996, with permission from Elsevier.

oriented microstructure of the natural tissues better than isotopically porous scaffolds [79−81]. Temperature gradient has been reported as a critical TIPS parameter in controlling the orientation of scaffold channels. For example, Wang et al. fabricated parallel microtubular channels in scaffolds by imposing a uniaxial temperature gradient on a PLGA/dioxane polymer solution constrained within a polyethylene mold [79]. Fig. 5.5 shows that scaffolds manufactured without a temperature gradient contained randomly distributed pores but those that were subjected to a gradient exhibited parallel microtubular pores. Moreover, gradient-derived TIPS scaffolds also possess anisotropic mechanical properties, in which their compressive modulus and yield strength are greater in the longitudinal direction than the transverse direction. Using human H144 cartilage cells as a model for in vitro biocompatibility testing, Wang showed that the cells were able to grow and migrate deeply into the microtubular pores of the anisotropic scaffold [79].

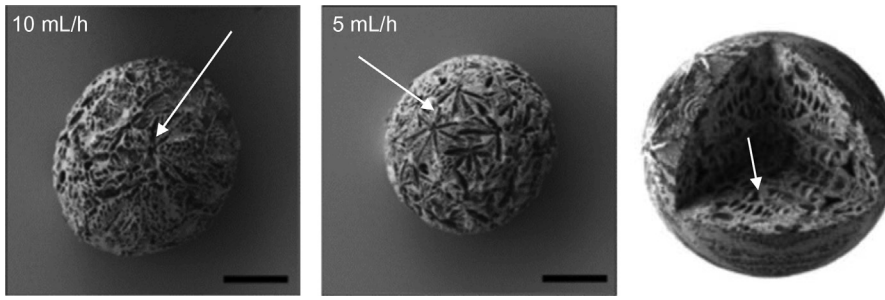

Figure 5.4 SEM images of TIPS PLGA microspheres fabricated using an electrospray technique. A) A transverse cross-section showing a lamellar pattern oriented around a central pore. B) Some of the inter-lamellar areas are subdivided into pores of approximately 10 μm. C) A longitudinal cross-section showing the elongated morphology of parallel lamellae. D) A higher magnification shows a uniform ladder-like morphology, highlighting the hierarchical nature of the foam.
Source: Reproduced from S.A. Malik, et al., Electrospray synthesis and properties of hierarchically structured PLGA TIPS microspheres for use as controlled release technologies, J. Colloid Interface Sci. 467 (2016) 220−229, Copyright 2006, with permission from Elsevier.

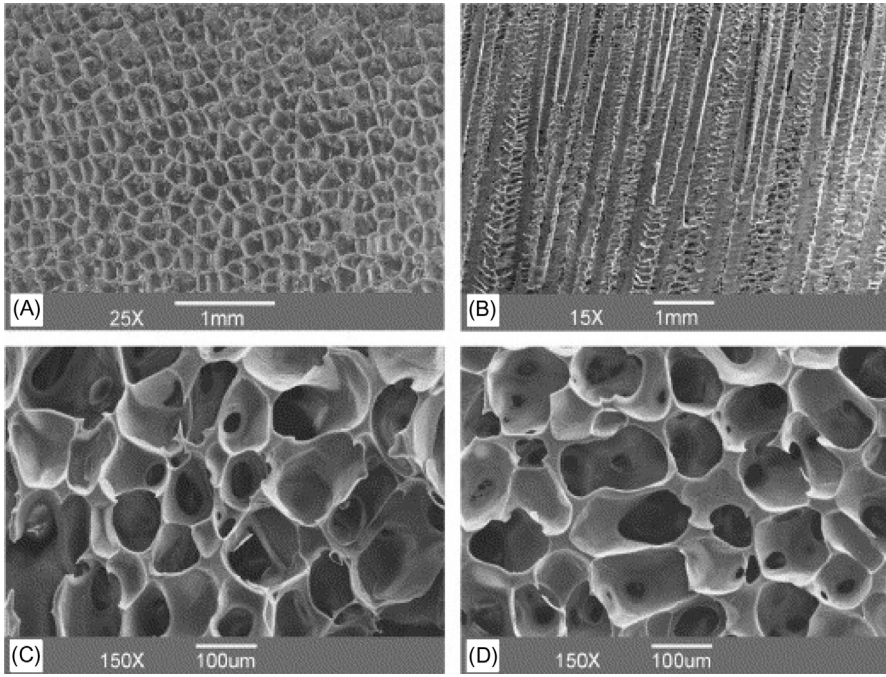

Figure 5.5 (A) Cross section and (B) longitudinal section of an orientation-structured PLGA scaffold produced from S−L phase separation with a temperature gradient. (C) cross section and (D) longitudinal section of a PLGA scaffold that was not treated with a gradient.
Source: Reproduced from F. Yang, et al., Manufacturing and morphology structure of polylactide-type microtubules orientation-structured scaffolds, Biomaterials 27 (28) (2006) 4923−4933, Copyright 2006, with permission from Elseiver.

The tissue scaffolds discussed so far are monolithic materials composed of only the polymer (after solvent extraction). However, studies have shown that composite scaffolds may be more advantageous in several aspects, including bioactivity and mechanical properties [27,82]. This is exemplified by the use of polymer/hydroxyapatite composite materials in bone tissue engineering [31]. Hydroxyapatite (HAP) is basically the inorganic component of natural bone tissues, making the mineral both biocompatible and osteoconductive [83,84]. Ma et al. [85] demonstrated that PLLA/HAP scaffolds fabricated using S−L phase separation have significantly higher compressive modulus and yield strength than pure PLLA foams.

To implement the characterization, PLLA/HAP/dioxane mixture was first cast into a cylindrical Teflon vial and phase separated to generate the composite as disks. The disks were then loaded onto a uniaxial mechanical tester for compressive modulus and yield strength measurements (Fig. 5.6). It was noted that the incorporation of HA particles also changed the typical structure of S−L phase separated materials. The characteristic channels became increasingly irregular as the HAP: polymer ratio was raised and this was likely due to the disruption of the solvent crystallization front by the HA particles [27]. In a different study carried out by Ma et al., the enhanced biocompatibility of PLLA/HAP composite scaffolds was reflected by the higher osteoblast (MC3T3-E1) cell number on them than pure PLLA scaffolds at all sampled time points throughout the in vitro cultivation period [85].

Histological analyses using von Kossa staining revealed that MC3T3-E1 cells were able to penetrate deep into the center of the PLLA/HAP scaffolds, but were sparser in the center of pure PLLA scaffolds (Fig. 5.7).

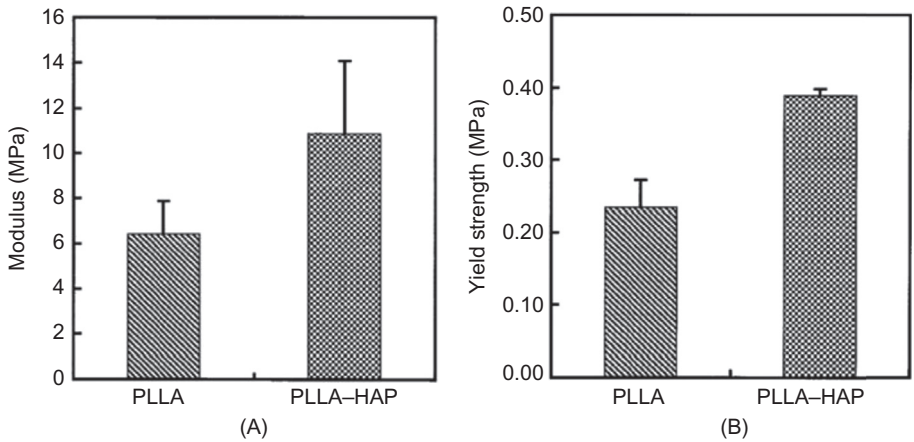

Figure 5.6 (A) Compressive modulus of PLLA scaffolds relative to that of PLLA/HAP scaffolds (B) Yield strength of PLLA and PLLA/HAP.
Source: Reproduced from R.Y. Zhang, P.X. Ma, Poly(alpha-hydroxyl acids) hydroxyapatite porous composites for bone-tissue engineering. I. Preparation and morphology, J. Biomed. Mater. Res. 44 (4) (1999) 446−455, Copyright 1999, with permission from John Wiley & Sons.

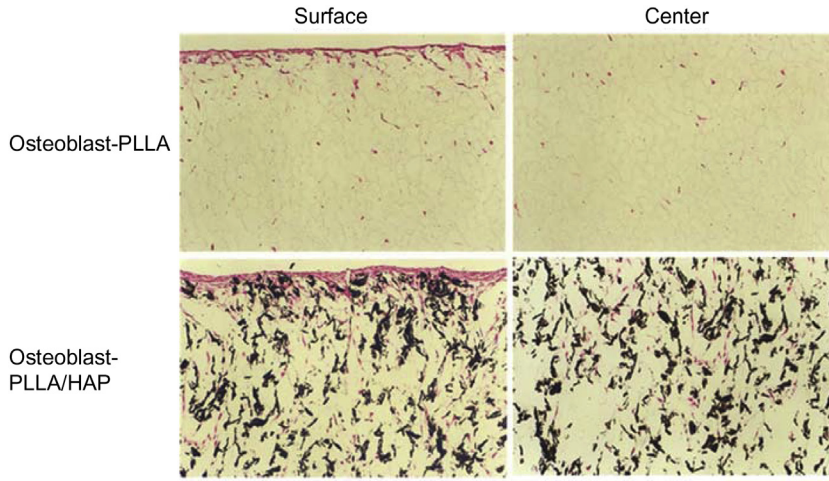

Figure 5.7 Osteoblast distribution in PLLA and PLLA/HAP scaffolds at 1 week post seeding. Cells with stained with von Kossa silver nitrate stain.
Source: Reproduced from P.X. Ma, et al., Engineering new bone tissue in vitro on highly porous poly (α-hydroxyl acids)/hydroxyapatite composite scaffolds. J. Biomed. Mater. Res. 54 (2) (2001) 284−293, Copyright 2000, with permission from John Wiley & Sons.

Furthermore, higher expression levels of bone-specific markers (mRNAs which code for bone sialoprotein and osteocalcin) were observed in the composite scaffolds than in pure PLLA scaffolds [85]. These findings point to the realization that despite the usefulness of S−L phase-separated materials in some of the aforementioned applications, their intrinsic functional properties may require further augmentation by bioactive materials to achieve optimal biomaterial-cell interaction for tissue engineering.

5.3.3 Applications of liquid−liquid phase separation

L−L phase separation can be employed to fabricate scaffolds with a nanofibrous morphology [30,86,87]. Such morphology has been found to be particularly useful in bone tissue engineering as it mimics the nanofibrous architecture of collagen (diameter $\approx$ 50−500 nm) in natural extracellular matrix (ECM) [86,88]. According to Ma et al., it is hypothesized that the nanofibers are generated when a polymer/solvent system undergoes L−L phase separation via spinodal decomposition and subsequent crystallization of the polymer-rich phase [88]. Here, it should be noted that the spinodal decomposition is also followed by a physical gelation process, which is considered crucial in generating ECM-like nanofibers [30]. It has been proposed that gelation causes the formation of physical crosslinks made of microcrystallites of the phase-separated polymer, which creates the 3D fibrous network after solvent extraction [52,88,89].

In his *Faraday Discussions* lecture, Keller provided a more detailed explanation of the mechanism behind different morphologies that result from a combination of thermally induced L−L phase separation and gelation/vitrification [90]. According to Keller, continual cooling during L−L phase separation will eventually cause the binodal line (Fig. 5.8E) intercept the lowered glass transition temperature at a point known as the Berghmans point. At this point, vitrification is initiated in the polymer-rich phase and L−L phase separation stops, meaning the morphology at that instant will get "frozen in." Therefore, the resultant scaffold morphology depends on the polymer−solvent interactions at the instant of vitrification.

Depending on the polymer concentration, different phase morphologies can be arrested in solution (Fig. 5.8A−D). At low polymer concentrations, small polymeric spheres will be formed. Intermediate concentrations generate a bicontinuous morphology of both phases—the polymer-lean phase will contribute to the pores after solvent extraction and the polymer rich phase will form physical networks upon vitrification (Fig. 5.8B). At high polymer concentrations, the polymer-lean phase will be dispersed in the polymer-rich matrix. It should be noted that the difference between the terms "gelation" and "vitrification" is not always clear—a discussion on whether vitrification and gelation should be treated as separate solidification processes is provided in Ref. [32].

He et al. fabricated both nanofibrous and platelet-like scaffolds by inducing L−L phase separation in a PLLA/dioxane/water system at different gelation temperatures [30]. In their study, 5% (w/v) PLLA was dissolved in 88/12 (v/v)

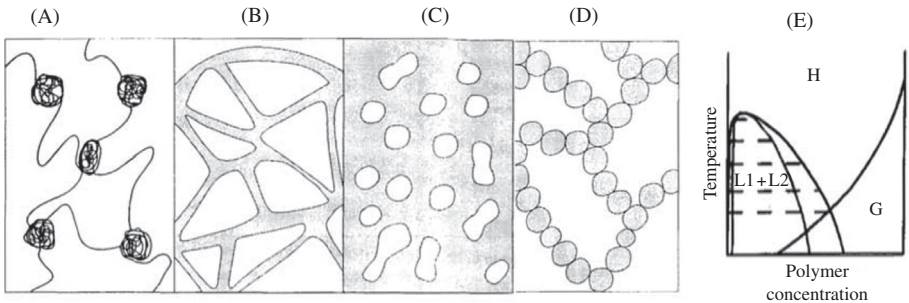

Figure 5.8 (A) Polymer rich phase (black) molecularly connected by solvated chains, (B) bi-continuous phase connected gel morphology, (C) glassy solid (phase connected), (D) disperse glassy phase connected through adhesive contact. (E) Phase diagram for L−L demixing and glass transition, where H, homogeneous solution; G, glassy state; L1, polymer-lean phase; and L2, polymer-rich phase. The outer solid line enclosing the L1 + L2 region is the binodal line.
Source: Panels (A−D) reproduced from A. Keller, Introductory lecture: aspects of polymer gels, Faraday Discuss. 101 (1995) 1−49, Copyright 1969, with permission from Royal Society of Chemistry. Panel (E) reproduced from P. Van de Witte, et al., Phase separation processes in polymer solutions in relation to membrane formation. J. Membr. Sci. 117 (1−2) (1996) 1−31, Copyright 1996, with permission from Elsevier.

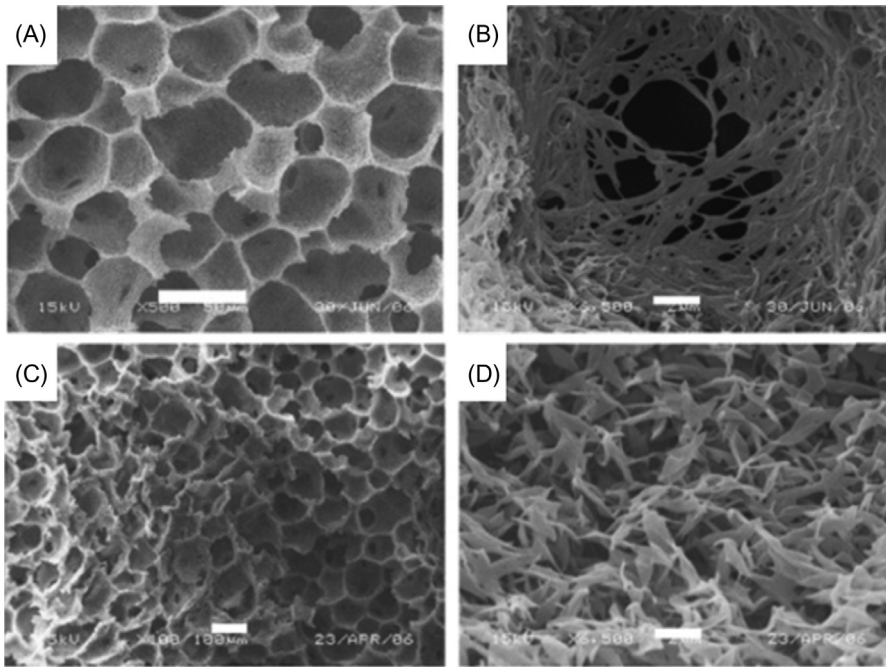

Figure 5.9 SEM images of PLLA scaffolds prepared at gelation temperatures of (A + B) 4°C and (C + D) 20°C.
Source: Reproduced from L. He, et al., Fabrication and characterization of poly(L-lactic acid) 3D nanofibrous scaffolds with controlled architecture by liquid−liquid phase separation from a ternary polymer−solvent system, Polymer (Guildf) 50 (16) (2009) 4128−4138, Copyright 2009, with permission from Elsevier.

dioxane/water and subsequently phase separated by quenching to different temperatures. All scaffolds were aged in the gel state for 2 hours before further processing to complete the fabrication procedure. It was found that at low gelation temperatures (below 12°C) walls of micropores/macropores were made of nanofibers (diameter = 50−200 nm), whereas only platelet-like structures were observed at 16 and 20°C (Fig. 5.9).

Similar results were also obtained by Ma et al. with a PLLA/tetrahydrofuran (THF) system [88]. The explanation provided by Ma on scaffold morphology is that the platelet structures are formed via a nucleation and growth mechanism, whereas spinodal decomposition is responsible for the fibrous network.

In terms of cell-biomaterial interactions, the fibrous scaffold made by He et al. consistently outperformed the platelet-structured scaffold in protein adhesion and maintaining viability (measured by methyl thiazolyl tetrazolium (MTT) assay) of rat-derived mesenchymal stem cells (MSCs) from 24 hours (post-seeding) onwards [30].

5.4 Conclusion

Phase-separation technologies provide an almost unrivaled platform for the manufacture of bespoke 3D tissue-engineering scaffolds. The manufacturing processes involved are often relatively low cost, scalable, and compatible with a wide range of materials. The structural features attained can be designed to resemble native extracellular matrix or provide novel substrates capable of stimulating specific cellular responses. These attributes are likely to result in the technology being increasingly utilized as the field of tissue engineering and regenerative medicine grows.

References

[1] S.H. Barbanti, C.A.C. Zavaglia, E.A.D.R. Duek, Effect of salt leaching on PCL and PLGA (50/50) resorbable scaffolds, Mater. Res. 11 (1) (2008) 75–80.
[2] D.R. Lloyd, K.E. Kinzer, H. Tseng, Microporous membrane formation via thermally induced phase separation. I. Solid-liquid phase separation, J. Membr. Sci. 52 (3) (1990) 239–261.
[3] Y. Cao, et al., The influence of architecture on degradation and tissue ingrowth into three-dimensional poly(lactic-co-glycolic acid) scaffolds in vitro and in vivo, Biomaterials 27 (14) (2006) 2854–2864.
[4] J.J. Blaker, J.C. Knowles, R.M. Day, Novel fabrication techniques to produce microspheres by thermally induced phase separation for tissue engineering and drug delivery, Acta Biomater. 4 (2) (2008) 264–272.
[5] N. Parmar, R. Ahmadi, R.M. Day, A novel method for differentiation of human mesenchymal stem cells into smooth muscle-like cells on clinically deliverable thermally induced phase separation microspheres, Tissue Eng. Part C. 21 (4) (2014) 404–412.
[6] H. Keshaw, et al., Assessment of polymer/bioactive glass-composite microporous spheres for tissue regeneration applications, Tissue Eng. Part A. 15 (7) (2008) 1451–1461.
[7] K.S. Foong, et al., Anti-tumor necrosis factor-alpha-loaded microspheres as a prospective novel treatment for Crohn's disease fistulae, Tissue Eng. Part C. 16 (5) (2010) 855–864.
[8] F.C. Pavia, et al., Polymeric scaffolds prepared via thermally induced phase separation: tuning of structure and morphology, J. Biomed. Mater. Res. A. 86 (2) (2008) 459–466.
[9] M. Sprenger, et al., Hierarchic structure formation in binary and ternary polymer blends, Interface Sci. 11 (2) (2003) 225–235.
[10] J.D. Van der Waals, P. Kohnstamm, Lehrbuch der Thermodynamik, vol. 2, Barth, 1912.
[11] P.J. Flory, Principles of Polymer Chemistry, Cornell University Press, 1953.
[12] M.L. Huggins, Theory of solutions of high polymers, J. Am. Chem. Soc. 64 (7) (1942) 1712–1719.
[13] H. Tompa, Phase relationships in polymer solutions, Trans. Faraday Soc. 45 (1949) 1142–1152.
[14] G.R. Brannock, D.R. Paul, Phase behavior of ternary polymer blends composed of three miscible binaries, Macromolecules 23 (25) (1990) 5240–5250.

[15] W.R. Burghardt, Phase diagrams for binary polymer systems exhibiting both crystallization and limited liquid-liquid miscibility, Macromolecules 22 (5) (1989) 2482–2486.
[16] A. Zakharov, Binary and ternary phase diagrams, Metallurgiya 1978 (1978) 295.
[17] C.H. Bamford, H. Tompa, The theory of coacervation, Trans. Faraday Soc. 46 (1950) 310–316.
[18] F.A.H. Schreinemakers, In-, Mono-, and Di-Variant Equilibria, Pennsylvania State University, 1965.
[19] R. Koningsveld, A.J. Staverman, Liquid–liquid phase separation in multicomponent polymer solutions. I. Statement of the problem and description of methods of calculation, J. Polym. Sci. Part A-2 6 (2) (1968) 305–323.
[20] Y.S. Nam, T.G. Park, Porous biodegradable polymeric scaffolds prepared by thermally induced phase separation, J. Biomed. Mater. Res. 47 (1) (1999) 8–17.
[21] R. Akbarzadeh, A.M. Yousefi, Effects of processing parameters in thermally induced phase separation technique on porous architecture of scaffolds for bone tissue engineering, J. Biomed. Mater. Res. B. 102 (6) (2014) 1304–1315.
[22] D.W. Hutmacher, Scaffold design and fabrication technologies for engineering tissues—state of the art and future perspectives, J. Biomater. Sci. Polym. Ed. 12 (1) (2001) 107–124.
[23] W.J. Li, R.S. Tuan, Fabrication and application of nanofibrous scaffolds in tissue engineering, Curr. Protoc. Cell Biol. (2009), Chapter 25:Unit 25.2.
[24] C.-Y. Chiang, D.R. Lloyd, Effects of process conditions on the formation of microporous membranes via solid-liquid thermally induced phase separation, J. Porous Mater. 2 (4) (2013) 273–285.
[25] B. Dhandayuthapani, et al., Polymeric scaffolds in tissue engineering application: a review, Int. J. Polym. Sci. 2011 (2011) 19.
[26] J.D. Kretlow, L. Klouda, A.G. Mikos, Injectable matrices and scaffolds for drug delivery in tissue engineering, Adv. Drug Deliv. Rev. 59 (4–5) (2007) 263–273.
[27] R.Y. Zhang, P.X. Ma, Poly(alpha-hydroxyl acids) hydroxyapatite porous composites for bone-tissue engineering. I. Preparation and morphology, J. Biomed. Mater. Res. 44 (4) (1999) 446–455.
[28] L. Budyanto, Y.Q. Goh, C.P. Ooi, Fabrication of porous poly(L-lactide) (PLLA) scaffolds for tissue engineering using liquid-liquid phase separation and freeze extraction, J. Mater. Sci. Mater. Med. 20 (1) (2009) 105–111.
[29] L. He, et al., Microstructural characteristics and crystallization behaviors of poly(l-lactide) scaffolds by thermally induced phase separation, J. Appl. Polym. Sci. 131 (4) (2014) 39436.
[30] L. He, et al., Fabrication and characterization of poly(l-lactic acid) 3D nanofibrous scaffolds with controlled architecture by liquid–liquid phase separation from a ternary polymer–solvent system, Polymer (Guildf) 50 (16) (2009) 4128–4138.
[31] G. Wei, P.X. Ma, Structure and properties of nano-hydroxyapatite/polymer composite scaffolds for bone tissue engineering, Biomaterials 25 (19) (2004) 4749–4757.
[32] P. Van de Witte, et al., Phase separation processes in polymer solutions in relation to membrane formation, J. Membr. Sci. 117 (1–2) (1996) 1–31.
[33] F.J. Hua, T.G. Park, D.S. Lee, A facile preparation of highly interconnected macroporous poly(D,L-lactic acid-co-glycolic acid) (PLGA) scaffolds by liquid–liquid phase separation of a PLGA–dioxane–water ternary system, Polymer (Guildf) 44 (6) (2003) 1911–1920.
[34] L. Budyanto, C.P. Ooi, Y.Q. Goh, Fabrication and characterization of porous poly(L-lactide) (PLLA) scaffolds using liquid-liquid phase separation, in: N.A. Abu Osman, et al. (Eds.), Fourth Kuala Lumpur International Conference on Biomedical

Engineering 2008: BIOMED 2008 25−28 June 2008 Kuala Lumpur, Malaysia, Springer Berlin Heidelberg, Berlin, Heidelberg, 2008, pp. 322−325.
[35] R. Chang, Physical Chemistry for the Biosciences, University Science Books, 2005.
[36] M.L. Huggins, Thermodynamic properties of solutions of long-chain compounds, Ann. N. Y. Acad. Sci. 43 (1) (1942) 1−32.
[37] P.J. Flory, Thermodynamics of high polymer solutions, J. Chem. Phys. 10 (1) (1942) 51−61.
[38] R. Koningsveld, A. Staverman, Liquid−liquid phase separation in multicomponent polymer solutions. II. The critical state, J. Polym. Sci., Part A-2 6 (2) (1968) 325−347.
[39] Y.C. Li, C.P. Wang, X.J. Liu, Thermodynamic assessments of binary phase diagrams in organic and polymeric systems, Calphad 33 (2) (2009) 415−419.
[40] D.R. Lloyd, S.S. Kim, K.E. Kinzer, Microporous membrane formation via thermally-induced phase separation. II. Liquid—liquid phase separation, J. Membr. Sci. 64 (1) (1991) 1−11.
[41] F.W. Altena, C. Smolders, Calculation of liquid-liquid phase separation in a ternary system of a polymer in a mixture of a solvent and a nonsolvent, Macromolecules 15 (6) (1982) 1491−1497.
[42] S.S. Kim, D.R. Lloyd, Thermodynamics of polymer/diluent systems for thermally induced phase separation: 1. Determination of equation of state parameters, Polymer (Guildf) 33 (5) (1992) 1026−1035.
[43] J.J. De Pablo, J.M. Prausnitz, Thermodynamics of liquid-liquid equilibria including the critical region, AIChE J. 34 (10) (1988) 1595−1606.
[44] S.S. Kim, D.R. Lloyd, Microporous membrane formation via thermally-induced phase separation. III. Effect of thermodynamic interactions on the structure of isotactic polypropylene membranes, J. Membr. Sci. 64 (1) (1991) 13−29.
[45] I.C. Sanchez, Polymer phase separation, in: A.R. Meyers (Ed.), Encyclopedia of Physical Science and Technology, Academic Press, New York, 1987, pp. 1−18.
[46] S.S. Kim, D.R. Lloyd, Thermodynamics of polymer/diluent systems for thermally induced phase separation: 2. Solid-liquid phase separation systems, Polymer (Guildf) 33 (5) (1992) 1036−1046.
[47] S.S. Kim, D.R. Lloyd, Thermodynamics of polymer/diluent systems for thermally induced phase separation: 3. Liquid-liquid phase separation systems, Polymer (Guildf) 33 (5) (1992) 1047−1057.
[48] T. Ishigami, et al., Solidification behavior of polymer solution during membrane preparation by thermally induced phase separation, Membranes 4 (1) (2014) 113−122.
[49] C. Schugens, et al., Biodegradable and macroporous polylactide implants for cell transplantation: 1. Preparation of macroporous polylactide supports by solid-liquid phase separation, Polymer (Guildf) 37 (6) (1996) 1027−1038.
[50] A.G. Mikos, J.S. Temenoff, Formation of highly porous biodegradable scaffolds for tissue engineering, Electron. J. Biotechnol. 3 (2) (2000) 6.
[51] Y.S. Nam, T.G. Park, Porous biodegradable polymeric scaffolds prepared by thermally induced phase separation, J. Biomed. Mater. Res. 47 (1) (1999) 8−17.
[52] F.J. Hua, et al., Macroporous poly(L-lactide) scaffold 1. Preparation of a macroporous scaffold by liquid--liquid phase separation of a PLLA--dioxane--water system, J. Biomed. Mater. Res. 63 (2) (2002) 161−167.
[53] C.A. Martínez-Pérez, et al., Scaffolds for tissue engineering via thermally induced phase separation, in: S. Wislet-Gendebien (Ed.), Advances in Regenerative Medicine, InTech, Croatia, 2011, pp. 275−294.

[54] F. Yang, et al., Fabrication of nano-structured porous PLLA scaffold intended for nerve tissue engineering, Biomaterials 25 (10) (2004) 1891–1900.
[55] J.I. Lim, H. Im, W.-K. Lee, Fabrication of porous chitosan-polyvinyl pyrrolidone scaffolds from a quaternary system via phase separation, J. Biomater. Sci. Polym. Ed. 26 (1) (2015) 32–41.
[56] R. Heijkants, et al., Design, synthesis and properties of a degradable polyurethane scaffold for meniscus regeneration, J. Mater. Sci. Mater. Med. 15 (4) (2004) 423–427.
[57] N. Zare-Mehrjardi, et al., Differentiation of embryonic stem cells into neural cells on 3D poly(D,L-lactic acid) scaffolds versus 2D cultures, Int. J. Artif. Organs 34 (10) (2011) 1012.
[58] T. Arahira, M. Todo, Effects of proliferation and differentiation of mesenchymal stem cells on compressive mechanical behavior of collagen/β-TCP composite scaffold, J. Mech. Behav. Biomed. Mater. 39 (2014) 218–230.
[59] A. Asefnejad, et al., Polyurethane/fluor-hydroxyapatite nanocomposite scaffolds for bone tissue engineering. Part I: morphological, physical, and mechanical characterization, Int. J. Nanomedicine 6 (1) (2011) 93–100.
[60] V. Maquet, et al., Porous poly (α-hydroxyacid)/Bioglass® composite scaffolds for bone tissue engineering. I: preparation and in vitro characterisation, Biomaterials 25 (18) (2004) 4185–4194.
[61] R.Y. Zhang, P.X. Ma, Porous poly(L-lactic acid)/apatite composites created by biomimetic process, J. Biomed. Mater. Res. 45 (4) (1999) 285–293.
[62] J.J. Blaker, et al., Mechanical properties of highly porous PDLLA/Bioglass® composite foams as scaffolds for bone tissue engineering, Acta Biomater. 1 (6) (2005) 643–652.
[63] M. Dziadek, et al., Effect of the preparation methods on architecture, crystallinity, hydrolytic degradation, bioactivity, and biocompatibility of PCL/bioglass composite scaffolds, J. Biomed. Mater. Res. B. 103 (8) (2015) 1580–1593.
[64] Y.Q. Goh, C.P. Ooi, Fabrication and characterization of porous poly(L-lactide) scaffolds using solid–liquid phase separation, J. Mater. Sci. Mater. Med. 19 (6) (2008) 2445–2452.
[65] S.A. Malik, et al., Electrospray synthesis and properties of hierarchically structured PLGA TIPS microspheres for use as controlled release technologies, J. Colloid Interface Sci. 467 (2016) 220–229.
[66] H. Keshaw, et al., Microporous collagen spheres produced via thermally induced phase separation for tissue regeneration, Acta Biomater. 6 (3) (2010) 1158–1166.
[67] N. Parmar, R.M. Day, TIPS to manipulate myogenesis: retention of myoblast differentiation capacity using microsphere culture, Eur. Cell. Mater. 30 (2015) 41–49, discussion 49–50.
[68] C. Sundback, et al., Manufacture of porous polymer nerve conduits by a novel low-pressure injection molding process, Biomaterials 24 (5) (2003) 819–830.
[69] J. Zhao, et al., Fabrication and in vivo osteogenesis of biomimetic poly(propylene carbonate) scaffold with nanofibrous chitosan network in macropores for bone tissue engineering, J. Mater. Sci. Mater. Med. 23 (2) (2012) 517–525.
[70] S. Wilbur, et al., Toxicological profile for 1,4-dioxane, Agency for Toxic Substances and Disease Registry (US), Health Advisory Atlanta, 2012.
[71] C.M. Murphy, M.G. Haugh, F.J. O'Brien, The effect of mean pore size on cell attachment, proliferation and migration in collagen–glycosaminoglycan scaffolds for bone tissue engineering, Biomaterials 31 (3) (2010) 461–466.
[72] L.G. Sicchieri, et al., Pore size regulates cell and tissue interactions with PLGA–CaP scaffolds used for bone engineering, J. Tissue Eng. Regen. Med. 6 (2) (2012) 155–162.

[73] S.M.M. Roosa, et al., The pore size of polycaprolactone scaffolds has limited influence on bone regeneration in an in vivo model, J. Biomed. Mater. Res. A. 92 (1) (2010) 359−368.
[74] W.L. Murphy, T.C. McDevitt, A.J. Engler, Materials as stem cell regulators, Nat. Mater. 13 (6) (2014) 547−557.
[75] F.J. O'brien, Biomaterials & scaffolds for tissue engineering, Mater. Today 14 (3) (2011) 88−95.
[76] S. Sundelacruz, D.L. Kaplan, Stem cell-and scaffold-based tissue engineering approaches to osteochondral regenerative medicine, Seminars in Cell & Developmental Biology, Elsevier, 2009.
[77] M.J. Song, D. Dean, M.L.K. Tate, Mechanical modulation of nascent stem cell lineage commitment in tissue engineering scaffolds, Biomaterials 34 (23) (2013) 5766−5775.
[78] H. Ghanbar, et al., Preparation of porous microsphere-scaffolds by electrohydrodynamic forming and thermally induced phase separation, Mater. Sci. Eng. C. 33 (5) (2013) 2488−2498.
[79] F. Yang, et al., Manufacturing and morphology structure of polylactide-type microtubules orientation-structured scaffolds, Biomaterials 27 (28) (2006) 4923−4933.
[80] P.X. Ma, R. Zhang, Microtubular architecture of biodegradable polymer scaffolds, J. Biomed. Mater. Res. 56 (4) (2001) 469−477.
[81] L. He, et al., Manufacture of PLGA multiple-channel conduits with precise hierarchical pore architectures and in vitro/vivo evaluation for spinal cord injury, Tissue Eng. Part C. 15 (2) (2009) 243−255.
[82] X. Liu, P.X. Ma, Polymeric scaffolds for bone tissue engineering, Ann. Biomed. Eng. 32 (3) (2004) 477−486.
[83] Z. Hong, et al., Nano-composite of poly(L-lactide) and surface grafted hydroxyapatite: mechanical properties and biocompatibility, Biomaterials 26 (32) (2005) 6296−6304.
[84] I. Smith, et al., Nanostructured polymer scaffolds for tissue engineering and regenerative medicine, Wiley Interdiscip. Rev. Nanomed. Nanobiotechnol. 1 (2) (2009) 226−236.
[85] P.X. Ma, et al., Engineering new bone tissue in vitro on highly porous poly(α-hydroxyl acids)/hydroxyapatite composite scaffolds, J. Biomed. Mater. Res. 54 (2) (2001) 284−293.
[86] J.M. Holzwarth, P.X. Ma, Biomimetic nanofibrous scaffolds for bone tissue engineering, Biomaterials 32 (36) (2011) 9622−9629.
[87] W. Zhang, et al., 3D porous poly(L-lactic acid) foams composed of nanofibers, nanofibrous microsheaves and microspheres and their application in oil-water separation, J. Mater. Chem. A. 3 (26) (2015) 14054−14062.
[88] P.X. Ma, R. Zhang, Synthetic nano-scale fibrous extracellular matrix, J. Biomed. Mater. Res. 46 (1) (1999) 60−72.
[89] J.K. Fink, Handbook of Engineering and Specialty Thermoplastics, Water Soluble Polymers, Wiley, 2011.
[90] A. Keller, Introductory lecture. Aspects of polymer gels, Faraday Discuss. 101 (1995) 1−49.